Eur J Appl Physiol (2010) 108:619–630
DOI 10.1007/s00421-009-1258-4

ORIGINAL ARTICLE

Effects of glutathione depletion and age on skeletal muscle performance and morphology following chronic stretch-shortening contraction exposure

Brent A. Baker · Melinda S. Hollander · Michael L. Kashon · Robert G. Cutlip

Accepted: 12 October 2009 / Published online: 31 October 2009
© Springer-Verlag 2009

Abstract The involvement of glutathione in the response of skeletal muscle following repetitive, high-intensity mechanical loading is not known. We examined the influence of a glutathione antagonist [L-Buthionine Sulfoximine (BSO)] had on the adaptability of skeletal muscle during chronic mechanical loading via stretch-shortening contractions (SSCs) in young and old rats. Left dorsiflexor muscles of young (12 weeks, $N = 16$) and old (30 months, $N = 16$), vehicle- and BSO-treated rats were exposed three times per week for 4.5-weeks to a protocol of 80 maximal SSCs per exposure in vivo. Skeletal muscle response to the SSC exposure was characterized by muscle performance, as well as muscle wet-weight and quantitative morphological analyses following the exposure period. Results reveal that generally, muscle performance increased in the young rats only following chronic SSC exposure. BSO treatment had no effect on muscle performance or morphology following the chronic SSC exposure in old rats. Muscle wet-weight was increased following exposure compared with the contra-lateral control limb, irrespective of age ($p < 0.05$). Muscle cross-sectional area increased approximately 20% with SSC loading in the young, vehicle rats, while increasing approximately 10% with SSC loading in old, vehicle rats compared with control rat muscle. No degenerative myofibers were noted in either age group, but edema were increased as a result of aging ($p < 0.05$). We conclude that our results indicate that glutathione depletion does not adversely affect muscle performance or morphology in old rats. Nevertheless, we continue to show that aging negatively influences performance and morphology following chronic SSC exposure.

Keywords Adaptation · Aging · Glutathione · Inflammation · Muscle hypertrophy · Stretch-shortening contractions

Communicated by Roberto Bottinelli.

The findings and conclusions in this report are those of the author(s) and do not necessarily represent the views of the National Institute for Occupational Safety and Health.

B. A. Baker · M. S. Hollander · M. L. Kashon · R. G. Cutlip (✉)
Health Effects Laboratory Division,
National Institute for Occupational Safety and Health,
1095 Don Nehlen Drive, M/S 2027,
Morgantown, WV 26505, USA
e-mail: rgc8@cdc.gov

Introduction

Increased oxidative stress in skeletal muscle following various modes of physical activity promotes cellular damage and loss of function (Zerba et al. 1990). We have previously demonstrated that the chronic exposure of young and old rats to stretch-shortening contractions (SSCs) does not necessarily produce skeletal muscle degeneration/necrosis, but results in adaptation in young rats and a maladaptive response in old rats (Cutlip et al. 2006). Further, aging may influence the adaptive/maladaptive response (defined by changes in muscle performance and muscle morphology) in old rats via unresolved, low-grade inflammation (Cutlip et al. 2006). Since oxidative stress production following high-intensity mechanical loading occurs along with changes in cellular responses (McBride et al. 1998) in aged skeletal muscle, it is possible that increased oxidative stress reduces the ability of muscles to adapt to SSC loading as well, especially in aged populations. Moreover, increased oxidative stress may also exacerbate the maladaptive response, so to contribute to an

injurious response manifested in skeletal muscle following mechanical loading/resistance-type training (Uchiyama et al. 2006). However, given that oxidative stress may also be an important stimulus for skeletal muscle adaptation (Urso and Clarkson 2003) in the absence of myofiber degeneration, modulating the oxidative stress profile and quantifying the resulting response may benefit our understanding with respect to optimizing mechanical-loading induced adaptations.

Glutathione, an important antioxidant and non-protein thiol source, is one mechanism maintaining cells in a reduced environment (Meister 1991), and serves various functions such as a reducing agent, a substrate for glutathione peroxidase, and recycling radicals generated from other antioxidant molecules. Because glutathione plays a major role in oxidant status, we modulated glutathione concentrations to determine if the adaptive capacity of skeletal muscle is under oxidant regulation. Glutathione can be depleted chronically using BSO, which is an irreversible inhibitor of γ-glutamylcysteine synthase (GCS) (Meister 1991; Leeuwenburgh and Ji 1995).

To assess skeletal muscle adaptation/maladaptation in young and old rats, we monitored changes in isometric and dynamic performance during a chronic 4.5-week exposure to SSCs. Following completion of the exposure, we also assessed morphological changes in skeletal muscle to determine if changes in performance were associated with changes in muscle morphology. Animals that have undergone glutathione depletion would be expected to be more vulnerable to mechanical loading-induced oxidative stress (Martensson and Meister 1989; Leeuwenburgh and Ji 1995). Our general hypothesis was that the glutathione acts to protect skeletal muscle from maladaptation (and subsequent muscle injury) and supports muscle adaptation and remodeling during chronic SSC loading. Thus, depleting glutathione via BSO will result in a failure of skeletal muscle to adapt to chronic SSC exposure in young rats. Further, because we previously demonstrated that old rats do not adapt to the SSC protocol administered in this study (Cutlip et al. 2006), we predicted that BSO treatment would exacerbate the effects of SSC exposure and increase indices of maladaptation or result in overt muscle injury in old rats.

Methods

Animal handling

We obtained male Fischer Brown Norway Hybrid rats (F344 × BN F1, $n = 32$) from the National Institutes on Aging colony, and housed young adult ($n = 16$; 3 months) and old ($n = 16$; 30 months) rats in an AAALAC accredited animal quarters. After 1 week of acclimatization, we randomly assigned young and old rats to BSO ($n = 6$), regular drinking water [vehicle, VEH ($n = 6$)], or cage-control groups [CON ($n = 4$)]. All animals, except those from the CON group, underwent exposure to a standardized experimental protocol approved by the NIOSH Animal Care and Use Committee. Temperature and light/dark cycle (dark cycle from 7.00 a.m. to 7.00 p.m.) remained constant for all animals; food and water were provided ad libitum for all groups, and water consumption was monitored for the experimental groups.

Glutathione depletion

Rats randomized to the BSO group received water with 10 mM BSO, beginning 3 days prior to the first exposure (Watanabe et al. 2003). All other groups received unsupplemented water. We noted no differences in water consumption during and after the exposure period with respect to age or treatment group. Preliminary data demonstrated that 10 mM BSO depleted total glutathione levels in tibialis anterior (TA) muscle homogenate to approximately 65% of control levels in old rats.

Experimental setup

We tested dorsiflexor muscles on a custom-built rodent dynamometer (Cutlip et al. 1997), which has been described in detail previously (Cutlip et al. 2004). Briefly, the dynamometer precisely controlled muscle length and muscle force output parameters. The software acquired and stored position, force, and velocity data in real-time as described elsewhere (Cutlip et al. 2004). We anesthetized the rats with 2% isoflurane gas using a small animal anesthetic system (Surgivet Anesco Inc., Waukesha, WI, USA) because it has no effect on in vivo force production (Ingalls et al. 1996). After anesthesia, we placed the rats supine on the heated *x-y* positioning table of the dynamometer with an anesthetic mask placed over the nose and mouth. We secured the knee in flexion (at 90°) with a knee holder, and the left foot in the load cell fixture using a custom-built foot holder with the ankle axis (assumed to be between the medial and lateral malleoli) aligned with the axis of rotation of the load cell fixture. We monitored each rat during the entire protocol to ensure proper anesthetic depth and body temperature.

Functional testing

With the experimental set-up, the functional testing has been described in detail previously (Cutlip et al. 2004). Briefly, we defined the joint position of the animal by the angle between the tibia and the plantar surface of the foot.

The angular position of the load cell fixture corresponded with the angular position of the ankle. We measured the force produced by the dorsiflexor muscles at the interface of the aluminum sleeve and the dorsum of the foot. We placed platinum stimulating electrodes (Grass Medical Instruments, Quincy, MA, USA) subcutaneously to span the peroneal nerve for activation via the electrical stimulator, which resulted in muscle contraction of the dorsiflexor muscle group. To reduce the effect of excitation–contraction fatigue, all electrical stimulation times were kept to a minimum with 2 min of recovery time between stimulations (Ingalls et al. 1998).

SSC protocol

We previously described the SSC protocol implemented in the current study in detail (Cutlip et al. 2006). Briefly, we exposed the dorsiflexor muscles of young and old experimental groups to 8 sets of 10 repetitions of SSCs with 2-min intervals between each set. Within each set, the muscles rested for 2 s between each stretch-shortening contraction. For each repetition, an electrical stimulator fully activated the dorsiflexor muscles for 100 ms, and the servomotor initiated the lengthening contraction phase with a 60 deg/s movement velocity of the load cell fixture over the prescribed range of motion of 90–140 deg ankle angle. The load cell fixture immediately returned in the concentric phase at 60 deg/s to the starting position of 90 deg ankle angle. The dorsiflexor muscles were deactivated 300 ms later with total stimulation time per repetition being 2.06 s. We administered the SSC protocol and performance tests three times per week for a total of 14 exposures over a 4.5 week period.

Isometric force test

We performed a pre-test isometric contraction (pre-test isometric force) and a post-test isometric contraction (post-test isometric force; executed immediately following the SSC protocol) on the dorsiflexor muscle group at an ankle angle of 90 deg using a 300 ms stimulation duration (Davis et al. 2003; Willems and Stauber 2001).

Dynamic force test

We measured a single SSC on the dorsiflexor muscle group 2 min preceding and following treatment with the SSC protocol as previously described (Cutlip et al. 2004). This test evaluated the muscle's ability to generate dynamic forces and to perform work during dynamic stretch-shortening. Work was calculated in the same fashion as previous work by Cutlip et al. (2004); Geronilla et al. (2003); Ettema (1996); Stevens and Faulkner (2000); and Stevens (Stevens 1996). We carried out the single SSC by activating the dorsiflexor muscles for 300 ms then moving the load cell fixture from 70 to 140 deg at an angular velocity of 500 deg/s. The load cell fixture immediately returned to 70 deg, at 500 deg/s, and activation continued for 300 ms after cessation of the movement.

Histology and immunohistochemistry (IHC)

Twenty-four hours after the final exposure, we weighed, anesthetized (sodium pentobarbital ip, 10 mg/100 g body weight) and exsanguinated the rats. We dissected and weighed the left (exposed: LTA) and right (contra-lateral control: RTA) tibialis anterior muscles. We then divided the muscle into five equally-sized "zones" ("Zone 1" most proximal–"Zone 5" most distal), mounted them onto cork board with OTC (VWR, West Chester, Pennsylvania), froze the sections in liquid nitrogen-cooled isopentane, and stored all mounted sections at −80°C. Samples rested for 3 min at room temperature prior to freeze fixation in isopentane cooled in liquid nitrogen. We selected "Zone 3" to obtain the maximum tissue sample corresponding to the TA mid-belly, and cut transverse sections at 12-μm thickness, mounted on pre-coated microscope slides, air dried, and stained with hematoxylin & eosin (H&E) using Harris' procedure. We assessed muscle morphology using standard stereological methods as used previously and described below. In addition, we used a glutathione primary antibody (Abcam Inc., Cambridge, MA, USA) and a fluorescently tagged secondary antibody (Cy3) and normal donkey serum for blocking (Jackson Immuno-Research Laboratories Inc., West Grove, PA) to localize and quantify total glutathione in TA muscle sections. Frozen sections used for glutathione immunolabeling that were stored at −80°C were fixed in ice cold acetone for 5 min and rinsed in PBS + 0.1 M Glycine for 5 min. We incubated slides in blocking buffer (5% normal donkey serum diluted in PBS + Triton X-100) at room temperature (RT) for 2 h. Next, we incubated slides in rabbit anti-glutathione antibody diluted in blocking buffer (1:100) for 1 h at 4°C, and following incubation, we rinsed slides in PBS and incubated for 1 h at RT in Cy3 labeled donkey anti-rabbit IgG (1:100). Finally, we rinsed slides, incubated in DAPI to stain nuclei (1:1,000, Sigma, St. Louis, MO, USA), coverslipped using Prolong Gold antifade reagent (Molecular Probes), and allowed to dry in a cool, dark area. We processed numerous slides in the absence of the primary antibody as controls for non-specific binding. Next, we captured photomicrographs using an Olympus Photomicroscope and Simple PCI Image Analysis Software. We quantified positively immunolabeled glutathione sections using one section per slide from the contra-lateral control RTA and exposed LTA muscles from each animal per

group. Then we obtained 20 non-overlapping digital images at 40× magnification using the mid-point of the section as a reference and stored these as raw images. Finally, we transformed the digital color images into grey-scale images and obtained the mean area grey values (mArGV) using Optimas Image Analysis Software.

Muscle quality

We normalized pre-test isometric force measured at the last session of the chronic exposure period to muscle wet-weight of the tibialis anterior of the exposed limb (Cutlip et al. 2006; Degens and Alway 2003).

Fiber cross-sectional area

For muscle fiber cross-sectional area (CSA) analysis, we obtained ten non-overlapping digital images from H&E-stained muscle sections at a 40× magnification and analyzed fiber CSA (μm^2) with Optimas Image Analysis Software. We traced approximately 200 fibers with a handheld mouse and calibrated the number of pixels inside the outlined region to a defined area in square micrometers (Cutlip et al. 2006).

Stereology

We used quantitative morphometric methods to measure the volume fraction, surface densities, and average thickness of normal myofibers, degenerative myofibers, and the interstitial space (Baker et al. 2006). The interstitium was divided into endomysial and perimysial spaces, which included capillaries. We used a standardized stereological technique (Baker et al. 2006) to quantify the degree of myofiber degeneration and inflammation, which was characterized as either non-cellular interstitium (NCI), indicative of edema, or cellular interstitium (CI), indicative of cellular infiltrates. We measured fiber volume and surface density using standard morphometric analyses (Weibel 1972, 1974, 1975; Underwood 1970). Briefly, we took one of the H&E stained sections from each animal to identify the mid-point of the section on a stage micrometer. Next, we recorded point and intercept counts using a 121-point/11-line overlay graticule (12.5 mm square with 100 divisions) at 40× magnification at five equally spaced points across the section, and repeated this process 2 mm on both sides of the mid-point of the section for a total of 1,210 points or 110 intercept lines per section. We computed volume density or percent volume from the percentage of points over the tissue section to points over normal myofibers, degenerative myofibers, cellular interstitium and non-cellular interstitium plus capillaries (Weibel 1972, 1974, 1975). We counted intercepts over the line overlay for the perimeter of normal myofibers, degenerative myofibers, and interstitium to myofiber transitions. Points and intercepts over blood vessels greater than 25 μm in diameter were excluded. We evaluated one section per animal per group. Further, we used stereology to quantify the degree of myofiber degeneration, and the accompanying changes in the TA muscle from each group. We defined myofibers by the following criteria. Normal myofibers demonstrated: (1) complete contact with adjacent myofibers, (2) a smooth outer membrane, and (3) no presence of internal inflammatory cells. Degenerative myofibers displayed: (1) a loss of contact with adjacent myofibers, (2) presence of internal inflammatory cells, and (3) an outer membrane interdigitated with inflammatory cells.

Data analysis

Analysis of glutathione IHC densitometry, stereological measures and muscle wet weight, normalized to tibia length, were analyzed using a three-way mixed model (treatment × age × limb) analyses of variance with the animal as the random factor to account for measures in both limbs. Muscle quality and isometric and dynamic force test measures including isometric force, F_{peak} (peak eccentric force), F_{min} (isometric pre-stretch force), negative work, and positive work, and the dynamic force parameters F_{peak} and F_{min} were calculated as previously described (Cutlip et al. 2006). These measures from exposure 1 and 2 as well as data from exposure 13 and 14 were averaged and these dependent variables were analyzed using a two-way analyses of variance with repeated measures (treatment × age). All data were analyzed using JMP v. 5.1 (SAS Institute Inc., Cary, NC, USA), and post-hoc comparisons were analyzed using Fishers LSD.

Results

Glutathione IHC

Treatment efficacy was analyzed using IHC on TA sections. Total glutathione levels decreased following BSO treatment in old rats ($p < 0.05$, Fig. 1) (CON RTA vs. BSO RTA) but not in young rats.

Isometric force

Dorsiflexor muscles from young and old rats generated similar magnitudes of isometric force prior to SSC exposure, regardless of treatment. The pre-test isometric force at the final exposure was not significantly different between the young and old age groups, however we noted a trend

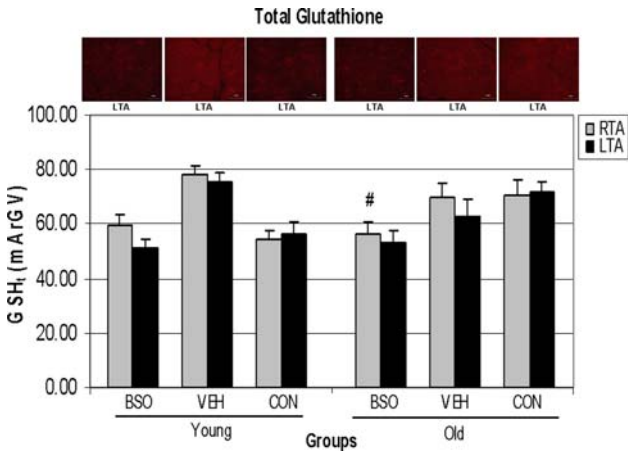

Fig. 1 Total glutathione levels reported as mArGV in young and old rats from BSO, VEH, and CON groups accompanied by representative immunolabeled micrographs from the exposed limb (labeled as LTA). RTA is the contra-lateral control limb and LTA is the SSC exposed limb. *Hash* represents significant effect of treatment when compared to CON RTA ($p < 0.05$). Data are reported as mean values ± SE

towards significance ($p = 0.08$, Fig. 2), with young rats producing 24.8% greater isometric force than their older counterparts, regardless of treatment.

Peak force (F_{peak})

Dorsiflexor muscle from young and old rats produced the same peak eccentric force prior to the first day of SSC exposure. However, by the end of the SSC exposures ($p < 0.05$, Fig. 3a), the dorsiflexor muscles from young rats produced significantly greater F_{peak} than their older counterparts. The increase in force induced by chronic SSC exposure resulted in an increase of F_{peak} in the young BSO- and VEH-treated rats following the exposure period ($p < 0.05$, Fig. 3b).

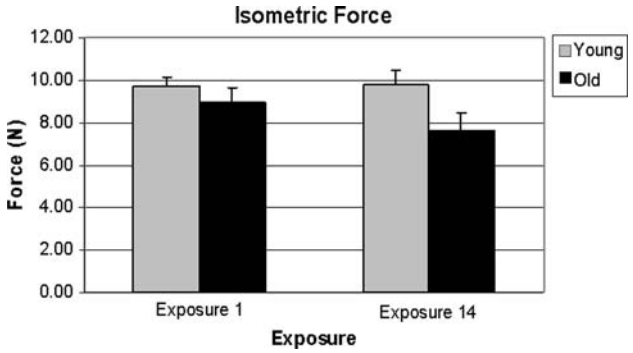

Fig. 2 Isometric force values for young and old rats exposed to 4.5 weeks of SSCs. Force values were not different preceding the initial SSC exposure, however we observed a trend ($p = 0.08$) for isometric force being increased in young rats compared with old rats following 4.5 weeks of SSC exposure. Data are reported as mean values ± SE

Minimum force (F_{min})

Following 4.5 weeks of SSC exposures, muscle from young rats' dorsiflexors produced greater F_{min} than dorsiflexors from old rats ($p < 0.05$, Fig. 3c), regardless of treatment.

Work

Age influenced the ability of the dorsiflexor muscles to absorb (negative work) and produce work (positive work). Treatment and age had no effect on the ability to absorb work prior to the first day of SSC exposure. However, age-related differences in the ability to absorb work occurred following 4.5 weeks of SSC exposures ($p < 0.05$, Fig. 4a). Young rats' dorsiflexors absorbed 21.6% more work than old rats at the conclusion of the exposure period. Specifically, negative work increased following 4.5 weeks of SSC exposure in the young BSO- and VEH-treated exposure ($p < 0.05$, Fig. 4b).

Unlike the observation for negative work, the ability to produce work differed with age prior to the first day of SSC exposure irrespective of treatment. Young rats' dorsiflexors produced significantly greater work than old rats ($p < 0.05$, Fig. 4c). After the 4.5 weeks of SSC exposures, the young rats' dorsiflexors produced 34.7% greater work than old rats.

Normalized muscle wet-weights

Overall, young rats had higher muscle wet-weights (normalized to tibia length) when compared to old rats, regardless of treatment ($p < 0.05$, Fig. 5). Following 4.5 weeks of exposure, muscle wet-weights from the exposed LTA were significantly increased compared the contra-lateral control RTA, irrespective of age or treatment ($p < 0.05$, Fig. 5).

Muscle quality

Regardless of treatment, old age decreased muscle quality (0.015 ± 0.0001 N/mg and 0.012 ± 0.0001 N/mg for the young group and old group, respectively). Young rats' dorsiflexors produced significantly greater isometric force normalized to muscle wet-weight in the exposed limb following 4.5 weeks of SSC exposure than old rats ($p = 0.05$, Fig. 6).

Stereological analyses of normal and degenerative myofibers

Old age decreased the volume density of normal myofibers compared to younger counterparts, regardless of treatment

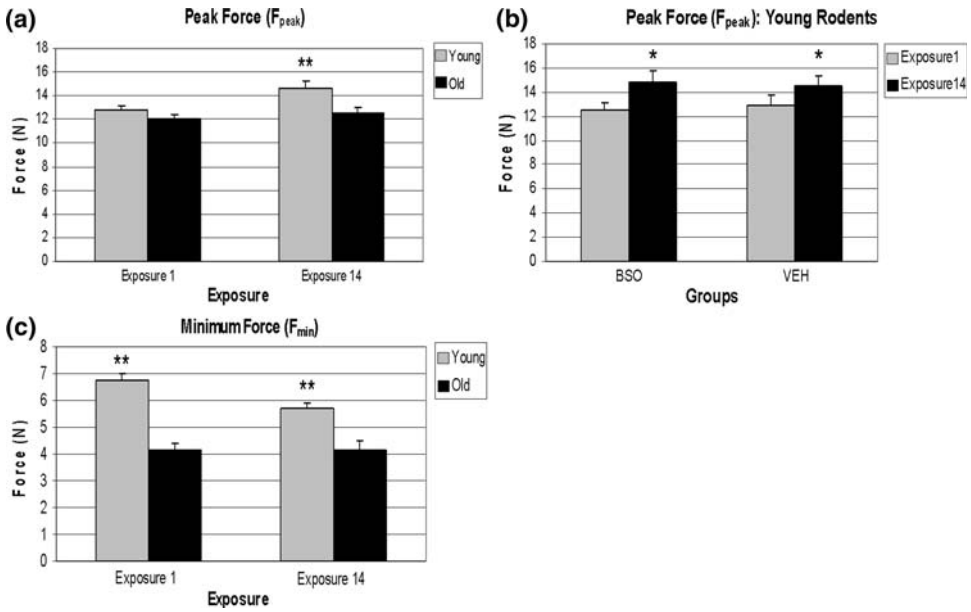

Fig. 3 Force parameters following SSC exposure. **a** Peak force (F_{peak}) of the young and old groups prior to and following 4.5 weeks of SSC exposures. Young rats displayed increased force following 4.5 weeks of SSC exposures compared with old rats. **b** Peak force (F_{peak}) of the young BSO and VEH groups was increased following 4.5 weeks of SSC exposures. *Significant effect of exposure ($p < 0.05$). **c** Minimum force (F_{min}) of young rats was increased compared with old rats prior to and following 4.5 weeks of SSC exposures. **Significant effect of aging ($p < 0.05$). Data are reported as mean values ± SE

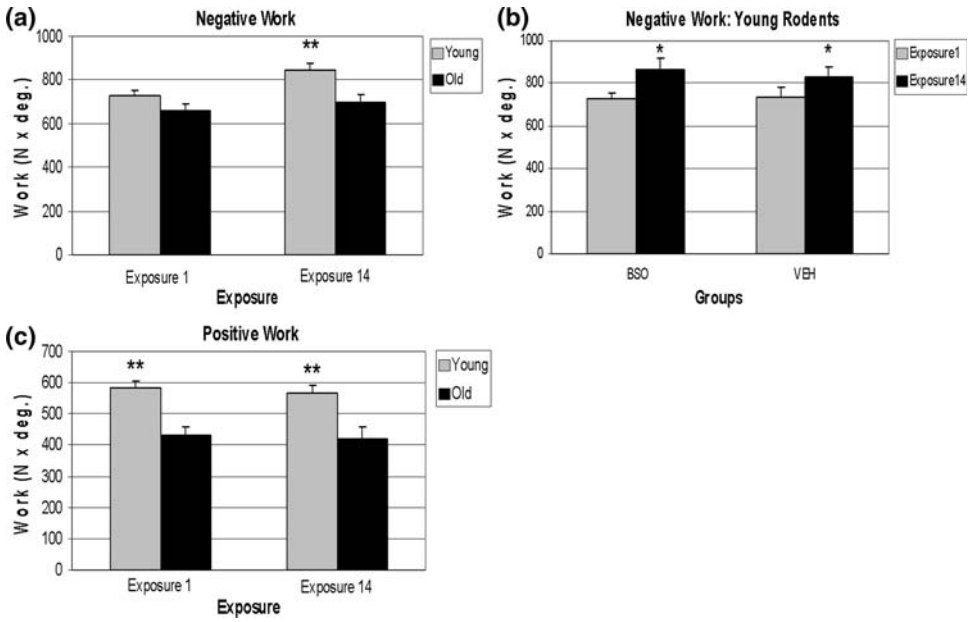

Fig. 4 Work parameters following SSC exposure. **a** The ability to absorb work (negative work) was greater in the young rats after 4.5 weeks of SSC exposures. **b** The ability to absorb work prior to the 1st day of SSC exposure and following 4.5 weeks of SSC exposures in the young BSO and VEH groups. **c** The ability to produce work (positive work) exhibited by the young and old rats prior to and following 4.5 weeks of SSC exposure. **Significant effect of aging ($p < 0.05$). Data are reported as mean values ± SE

or limb ($p < 0.001$, Fig. 7a). Additionally, BSO treatment led to a decrease in the volume density of normal myofibers in all rats ($p < 0.05$, Fig. 7b). No degenerative myofibers presented in muscle samples analyzed from any groups.

Stereological analyses of inflammation

Aging increased the volume density of NCI, indicative of edema, compared to young counterparts, regardless of treatment or limb ($p < 0.001$, Fig. 7c). Further, BSO-treated rats displayed increased NCI when compared to cage-control rats, as age and limb had no effect ($p < 0.05$, Fig. 7d). Aging did not influence the response of cellular interstitium, indicative of cellular infiltrates.

Fiber cross-sectional area

Cross-sectional area (CSA) data from young CON rats showed that approximately 46% of RTA and 48% of LTA muscle fibers were ≥2,000 μm^2. CSA data from the old CON rats revealed similar results: approximately 50% of RTA and 46% of LTA muscle fibers were ≥2,000 um^2. Thus, we established all myofibers ≥2,000 μm^2 as being our qualitative hypertrophic threshold.

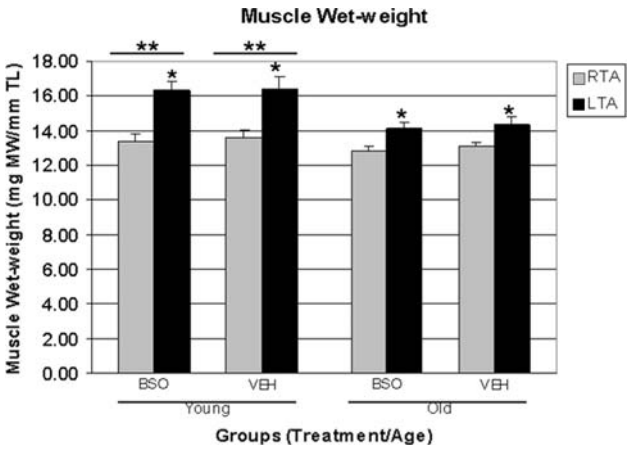

Fig. 5 Exposure to SSCs increased normalized muscle wet-weight in the LTA in young and old rats. Adjusted muscle weights were higher in young compared with old rats. *Significant effect of limb ($p < 0.05$). **Significant effect of aging ($p < 0.05$). Data are reported as mean values ± SE

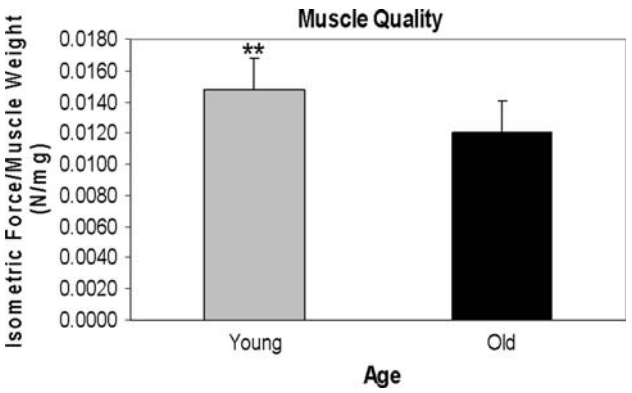

Fig. 6 Pre-test isometric force measured at the last SSC exposure was normalized to muscle wet-weight of the tibialis anterior for young and old rats following 4.5 weeks of SSC exposure (N/mg). **Significant effect of aging ($p = 0.05$). Data are reported as mean values ± SE

Representative sections from the young, VEH-treated exposed LTA (Fig. 8a) depict normal morphology and larger fibers, indicative of hypertrophy, when compared the corresponding young VEH-treated control RTA (Fig. 8b). The muscle sections from the old, VEH-treated exposed LTA (Fig. 8c) depicted fibers with a blunted hypertrophic response and evidence of mild cellular infiltrates that was not evident in the samples from the old VEH-treated control RTA (Fig. 8d). BSO-treated sections presented with results similar to VEH-treated samples for both LTA and RTA (Fig. 9a–d), with the exception being that old, BSO-treated LTA did not show evidence of cellular infiltrates.

In the unexposed RTA, approximately 50% of the fibers from the old, VEH-treated rats and 47% of the fibers from the young, VEH-treated rats were ≥2,000 μm^2 (Fig. 10a). In the exposed LTA, approximately 61% of the fibers from the old, VEH-treated animals and 65% of the fibers from the young, VEH-treated rats were ≥2,000 μm^2 (Fig. 10b). Overall, RTA and LTA muscle fiber histograms were similar for the BSO-treated rats compared with VEH-treated groups (Figs. 10c, d, respectively).

Discussion

In the present investigation we, once again, report increased performance and hypertrophy in rats following SSC exposure and demonstrate that glutathione depletion does not negatively influence this outcome; however this response is blunted in old rodents. Surprisingly, an increase in cellular infiltrates was not present [this is in contrast to what we have previously reported in old rats (Cutlip et al. 2006)], although a trend did exist in the old rats for increased cellular infiltrates. It was hypothesized that depleting the host environment of glutathione would increase oxidative stress in young rats, and aging would intensify this response due to the damaging and cumulative effects of ROS that evolve over time (Bejma and Ji 1999). However, we have shown that old rats' do not display a greater decrease in performance or dramatic change in morphology when exposed to chronic SSCs in the presence of glutathione depletion compared with exposure alone. We acknowledge that a limitation to the interpretation of the current data is our inability to show treatment efficacy for the young BSO-treated rodents using the immunohistochemical technique in the current study. In spite of this, we successfully showed that old BSO-treated rats did have decreased levels of total glutathione in skeletal muscle following treatment, yet this did not impact the functional or morphological response we observed for this group compared with the old VEH-treated group. Thus, one would expect that if glutathione depletion was detrimental to performance and morphology it would be observed with increased age, yet our old rats did not exhibit any unfavorable response following BSO treatment. Furthermore, to our knowledge, this is the first time that total glutathione has been localized and quantified in skeletal muscle using this immunohistochemical technique. Because performance and morphological changes may be achieved by specifically and selectively conserving glutathione in metabolically active tissue and allowing for maintenance of increased oxidative stress (Leeuwenburgh and Ji 1995) or by compensatory mechanisms (increases in other antioxidant systems) following glutathione depletion, this may be an explanation for not observing a decrease in glutathione levels in young rats. Thus, we suggest that glutathione depletion in old rats exposed to high-intensity mechanical loading via SSC exposure does not directly induce a maladaptive state and/or that glutathione is not critical for SSC-loading adaptation.

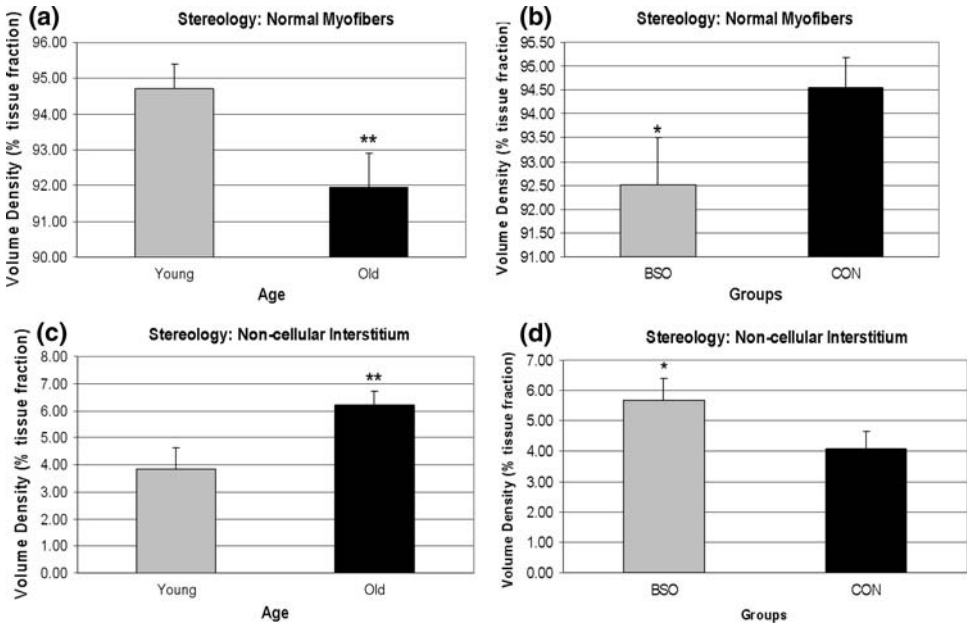

Fig. 7 The volume density (% tissue fraction) of normal myofibers in the young and old rats (**a**) and BSO and CON rats (**b**). **c**, **d** The volume density (% tissue fraction) of non-cellular interstitium (NCI) in the young and old rats (**c**) and BSO and CON rats (**d**). *Significant effect of treatment ($p < 0.05$). **Significant effect of aging ($p < 0.001$). Data are reported as mean values ± SE

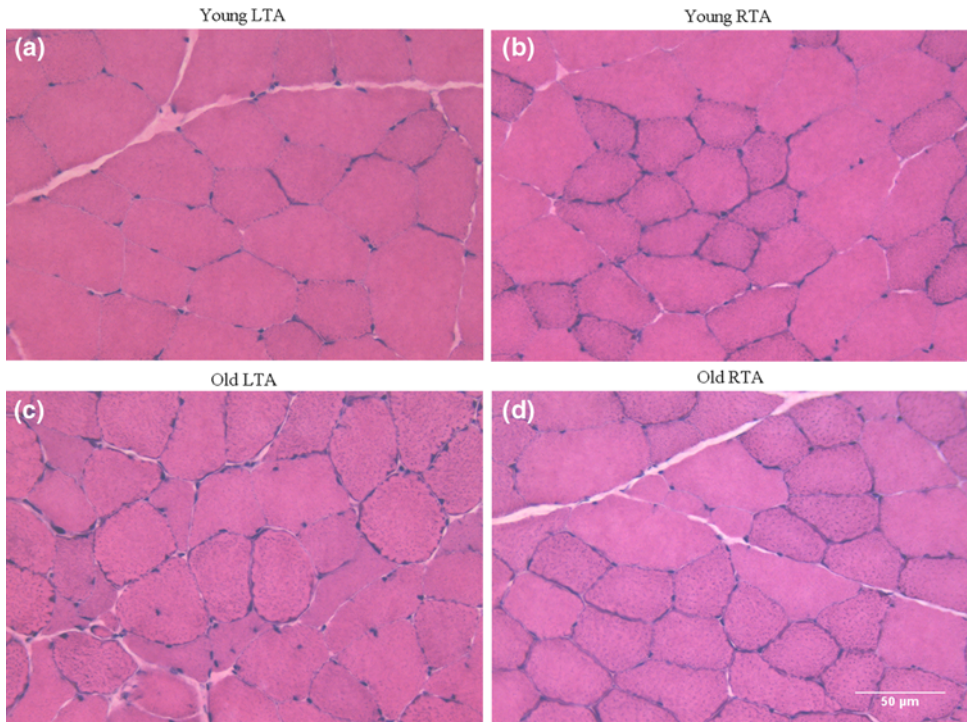

Fig. 8 Hematoxylin and eosin stained sections of the exposed LTA and contra-lateral control RTA muscle from young, vehicle-treated (**a**, **b**) and old, vehicle-treated rats (**c**, **d**), respectively. All micrographs shown are representative of the overall groups and are captured at 40× magnification

The differences observed with respect to isometric and dynamic performance measure prior to and following 1 and 14 SSC exposures in the current investigation compared with those published recently by our lab (Cutlip et al. 2006), may be the result of the variation we observed in the size of the TA muscle fibers. Previously, our morphometric data showed that young and old Fischer Hybrid rodent TA muscle fibers (of the same age in the current study) were smaller in size. This may account for the disparity we observed between both the initial force generating capacity of the rats in this study, as well as the adaptive/maladaptive response to exposure. The exposure paradigm used in the current study resulted in an increase of 4.2% for the average isometric force above the pre-test force in young, VEH-treated rats, while producing a 12.9% deficit in old, VEH-treated rats. The same general response was observed in the young and old rats receiving BSO treatment with respect to isometric performance. Whether a chronic increase in non-cellular interstitium promotes an environment that

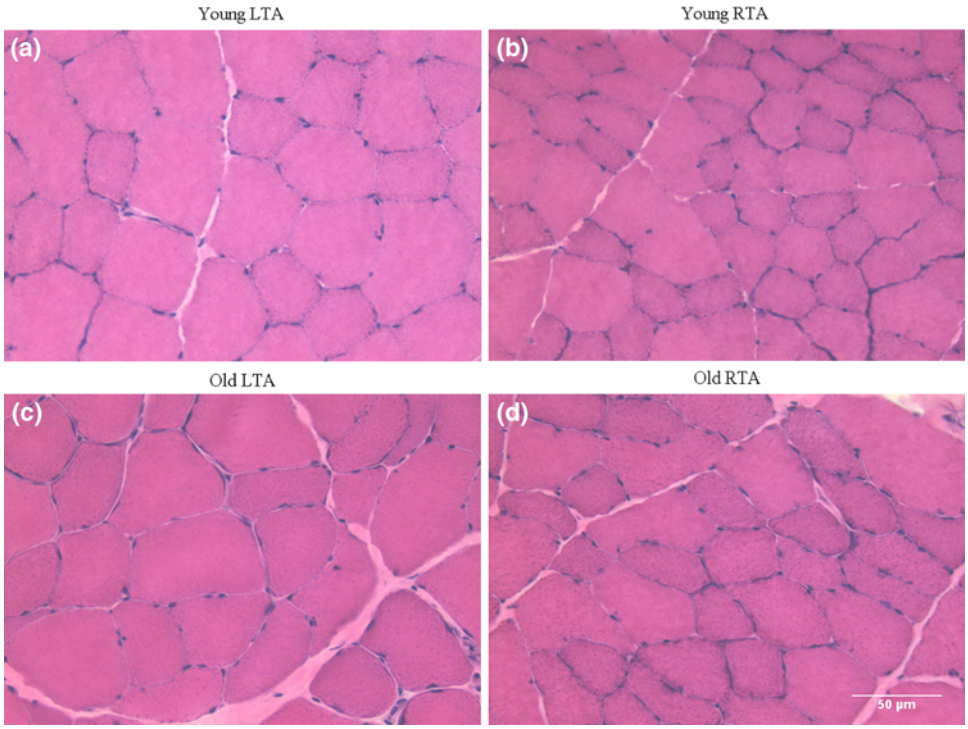

Fig. 9 Hematoxylin and eosin stained sections of the exposed LTA and contra-lateral control RTA muscle from young, BSO-treated (**a**, **b**) and old, BSO-treated rats (**c**, **d**), respectively. All micrographs shown are representative of the overall groups and are captured at 40× magnification

aggravates long-term cellular signaling leading to functional deficits is not known. Here, we show that estimates of edema were increased in old rats following SSC loading. Thus, unresolved permeability changes may have contributed to the decreased functional performance at this time. It is plausible that chronic alterations in cellular permeability with increased age may contribute to long-term maladaptation by modifying the local internal environment and ultimately affect muscle remodeling. Previous investigations support this hypothesis, because alterations in the host environment's systemic factors with aging have been shown to adversely affect local tissue repair and regeneration (Conboy et al. 2005), which ultimately may affect function. Alternatively, age-related excitation–contraction (EC) coupling concurrent with calcium signaling and handling dysregulation has been indicated to affect specific force in single muscle fibers (Gonzalez et al. 2000). However, these events would manifest as early events (24–48 h) following the mechanical exposure, which we did not observe. Thus, although the role of calcium cannot be dismissed, a more appropriate means in which to consider EC coupling's impact on performance with aging is that mechanical perturbation causes alterations and fragility of the transverse tubules (t-tubules) and associated receptor complexes (Payne and Delbono 2004) that may lead to decreased transmission efficiency. Furthermore, alterations in actin-myosin contractile proteins involved in cross-bridge cycling have been shown to contribute to an age-related decline in specific force (Lowe et al. 2002). Thus, these events may also influence the age-related decline in isometric and dynamic performance we observed in the current study. Furthermore, peak eccentric force increased in both the young, VEH-treated (12.1%) and young, BSO-treated (17.9%) rats but did not increase in the old, VEH- or BSO-treated rats. The data reported here for our VEH rats are in general agreement with Brooks et al. (2001) who reported a significant increase in peak force by week 6 of exposure for both adult and old animals over baseline values in mice. Disparities between our current performance data and that which has been reported previously may be related to differences between and within species and/or strains, as well as to differences we have noted with respect to muscle fiber size heterogeneity within this strain.

Changes in degenerative myofibers and cellular infiltrates were not significant following the terminal session in the current study, but changes in non-cellular interstitium, indicative of edema, in the muscles of old rats were significant. Further, degeneration and cellular interstitium were not influenced by glutathione depletion, even though estimates of edema were increased in BSO-treated rats. Collectively, the precise composition and magnitude of the general exposure response (degeneration, inflammation, and swelling) may be an important factor in signaling skeletal muscle adaptation (Tidball 2005). Thus, our data continues to indicate that the modifications made to the interstitial space are critical for adaptation, and the inability

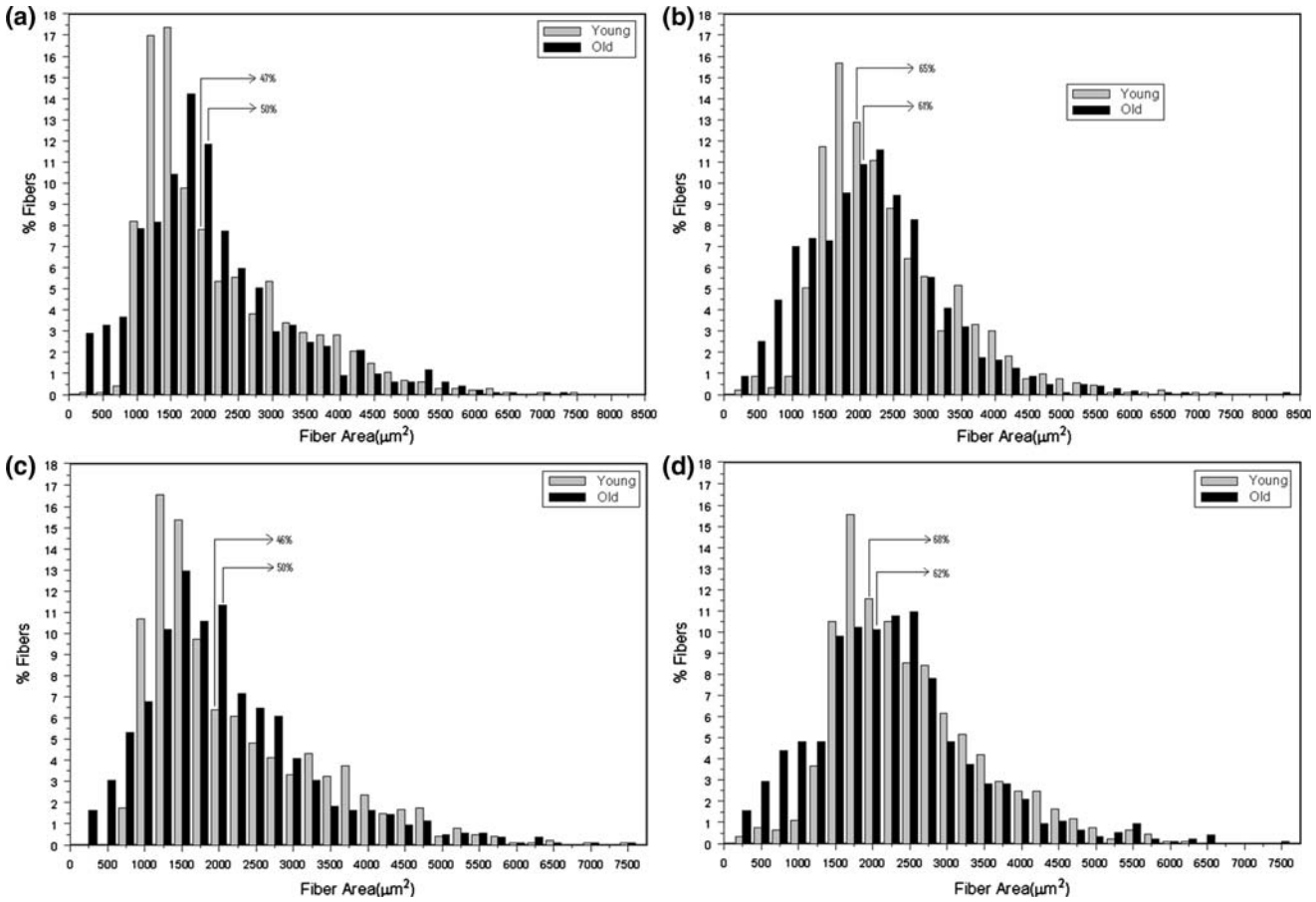

Fig. 10 **a** Mean cross-sectional area (CSA, μm^2) distribution in young and old VEH-treated contra-lateral control RTA muscle. The frequency histogram depicts the frequency of fibers, which lie above/below 2,000 μm^2. Approximately 50% of the fibers from the older rats and 47% of the fibers from the younger rats were $\geq$2,000 μm^2. **b** Mean cross-sectional area (CSA, μm^2) distribution in young and old VEH-treated exposed LTA muscle. Approximately 61% of the fibers from the older rats and 65% of the fibers from the younger rats were $\geq$2,000 μm^2. **c** Mean cross-sectional area (CSA, μm^2) distribution in young and old BSO-treated contra-lateral control RTA muscle. Approximately 50% of the fibers from the older rats and 46% of the fibers from the younger rats were $\geq$2,000 μm^2. **d** Mean cross-sectional area (CSA, μm^2) distribution in young and old BSO-treated exposed LTA muscle. Approximately 62% of the fibers from the older rats and 68% of the fibers from the younger rats were $\geq$2,000 μm^2. Regardless of treatment, note the existing population of small fibers ($\leq$1,000 μm^2) in the old rodent's muscle

of old rats to fully adapt may be influenced by the internal host environment as hypothesized by others (Conboy et al. 2005). Furthermore, the modest morphological changes observed in old rats may have resulted from attenuation of the cellular interstitial response that we have recently reported (Cutlip et al. 2006). By decreasing the percent volume fraction of cellular interstitium, a more favorable host environment may have resulted in terms of permitting skeletal muscle adaptation. Nonetheless, we are again reporting the absence of degenerative myofibers following high-intensity mechanical loading, which supports a recent investigation from our lab (Cutlip et al. 2006), where the exposed muscles of rats did not exhibit myofiber degeneration. This may validate our hypothesis that not all high-intensity mechanical loading leads to overt skeletal muscle degeneration.

The data in the present study clearly show that SSC loading increases muscle mass in young rats, and that this response was diminished in old rats. The increase in muscle wet-weight could have resulted from and be attributed to chronic edema, but based on our findings, we do not believe this is the case. Results from our muscle cross-sectional area data support the observation that there was myofiber hypertrophy in the young, exposed rats as evidenced by a shift to larger fibers. Despite previous reports that indicate skeletal muscles in old animals are more susceptible to injury (Brooks and Faulkner 1996; Zerba et al. 1990), and recover more slowly (McBride et al. 1995; Brooks and Faulkner, 1990) from a single exposure to injurious contractions, there is evidence that old animals can be conditioned for protection from contraction-induced myofiber injury (Brooks

et al. 2001). Muscle hypertrophy and improvements in force production occur in response to constant or chronic loading in aged animals, although the extent of muscle enlargement is attenuated relative to young animals (Alway 1995; Alway et al. 2002; Carson et al. 1995; Klitgaard et al. 1989a, b, Lowe et al. 1998). Since myofiber cross sectional area and stereology data from the contra-lateral limbs of both groups were not different, this suggests that there was not a different systemic response. The lack of myofiber degeneration in the exposed limbs of the old rats suggests that the decreased functional capacity observed in the TA muscle is not due to fiber degeneration, but necessitates future research into the causal factors influencing muscle structure–function relationships within aging populations.

In addition to age, several other factors may explain the difference in performance, physiological, and morphological measures between the two groups during the current chronic exposure and differences observed in a recent study from our lab (Cutlip et al. 2006). (1) The mode of exposure may significantly contribute to changes observed following repetitive exposure (anaerobic versus aerobic exposures). (2) The older animals may not have tolerated the repeated exposure to isoflurane as well as their younger counterparts, which could have affected contractile performance. (3) However, performance data clearly show that old rats have a limited capacity to adapt and that an alternate explanation to the differences observed may be influenced by inherent variability within or between cohorts of an animal strain or between species examined. As mentioned above, we have recently demonstrated that old rat's do not adapt to the identical exposure paradigm functionally, physiologically, and morphologically. In the current study obvious maladaptation, which was observed previously (Cutlip et al. 2006), was not as striking.

Our findings suggest that glutathione depletion in old rats exposed to chronic SSCs does not induce an overt maladaptive state; however we continue to show that aging negatively influences performance and morphology following chronic SSC exposure when compared to young counterparts. Yet, we are unable to rule out completely the involvement of other oxidative pathways that may be influential in producing adaptation/maladaptation following chronic SSC exposures. Isolating elements that impact cellular signaling such as increased oxidative stress, inflammation, and/or edema in skeletal muscle under repetitive high-intensity mechanical loading that may influence the response of the oxidant/antioxidant profile continues to be of major importance when designing preventative strategies that attenuate muscular maladaptation in workplace and recreational settings.

Acknowledgments The authors would like to thank Drs. Paul Nicolaysen, Kristine Krajnak, and Pius Joseph of the National Institute for Occupational Safety and Health (NIOSH) for their critical review and comments regarding the preparation manuscript.

References

Alway SE (1995) Slowing of contractile properties in quail skeletal muscle with aging. J Gerontol A Biol Sci Med Sci 50A:B26–B33

Alway SE, Degens H, Krishnamurthy G, Smith CA (2002) Potential role for Id myogenic repressors in apoptosis and attenuation of hypertrophy in muscles of aged rats. Am J Physiol Cell Physiol 283:C66–C76

Baker BA, Mercer RR, Geronilla KB, Kashon ML, Miller GR, Cutlip RG (2006) Stereological analysis of muscle morphology following exposure to repetitive stretch-shortening cycles in a rat model. Appl Physiol Nutr Metab 31:167–179

Bejma J, JI LL (1999) Aging and acute exercise enhance free radical generation in rat skeletal muscle. J Appl Physiol 87:465–470

Brooks SV, Faulkner JA (1990) Contraction-induced injury: recovery of skeletal muscles in young and old mice. Am J Physiol 258:C436–C442

Brooks SV, Faulkner JA (1996) The magnitude of the initial injury induced by stretches of maximally activated muscle fibres of mice and rats increases in old age. J Physiol 497(Pt 2):573–580

Brooks SV, Opiteck JA, Faulkner JA (2001) Conditioning of skeletal muscles in adult and old mice for protection from contraction-induced injury. J Gerontol A Biol Sci Med Sci 56:B163–B171

Carson JA, Alway SE, Yamaguchi M (1995) Time course of hypertrophic adaptations of the anterior latissimus dorsi muscle to stretch overload in aged Japanese quail. J Gerontol A Biol Sci Med Sci 50:B391–B398

Conboy IM, Conboy MJ, Wagers AJ, Girma ER, Weissman IL, Rando TA (2005) Rejuvenation of aged progenitor cells by exposure to a young systemic environment. Nature 433:760–764

Cutlip RG, Stauber WT, Willison RH, Mcintosh TA, Means KH (1997) Dynamometer for rat plantar flexor muscles in vivo. Med Biol Eng Comput 35:540–543

Cutlip RG, Geronilla KB, Baker BA, Kashon ML, Miller GR, Schopper AW (2004) Impact of muscle length during stretch-shortening contractions on real-time and temporal muscle performance measures in rats in vivo. J Appl Physiol 96:507–516

Cutlip RG, Baker BA, Geronilla KB, Mercer RR, Kashon ML, Miller GR, Murlasits ZS, Alway SE (2006) Chronic exposure to stretch-shortening contractions results in skeletal muscle adaptation in young rats and maladaptation in old rats. Appl Physiol Nutr Metab 31:573–587

Davis J, Kaufman KR, Lieber RL (2003) Correlation between active and passive isometric force and intramuscular pressure in the isolated rabbit tibialis anterior muscle. J Biomech 36:505–512

Degens H, Alway SE (2003) Skeletal muscle function and hypertrophy are diminished in old age. Muscle Nerve 27:339–347

Ettema GJ (1996) Mechanical efficiency and efficiency of storage and release of series elastic energy in skeletal muscle during stretch-shorten cycles. J Exp Biol 199(Pt 9):1983–1997

Geronilla KB, Miller GR, Mowrey KF, Wu JZ, Kashon ML, Brumbaugh K, Reynolds J, Hubbs A, Cutlip RG (2003) Dynamic force responses of skeletal muscle during stretch-shortening cycles. Eur J Appl Physiol 90:144–153

Gonzalez E, Messi M, Delbono O (2000) Contractile properties of single intact mouse extensor digitorum longus (EDL), flexor digitorum brevis (FDB) and soleus muscle fibers. J Memb Biol 178:175–183

Ingalls CP, Warren GL, Lowe DA, Boorstein DB, Armstrong RB (1996) Differential effects of anesthetics on in vivo skeletal muscle contractile function in the mouse. J Appl Physiol 80:332–340

Ingalls CP, Warren GL, Williams JH, Ward CW, Armstrong RB (1998) E-C coupling failure in mouse EDL muscle after in vivo eccentric contractions. J Appl Physiol 85:58–67

Klitgaard H, Brunet A, Maton B, Lamaziere C, Lesty C, Monod H (1989a) Morphological and biochemical changes in old rat muscles: effect of increased use. J Appl Physiol 67:1409–1417

Klitgaard H, Marc R, Brunet A, Vandewalle H, Monod H (1989b) Contractile properties of old rat muscles: effect of increased use. J Appl Physiol 67:1401–1408

Leeuwenburgh C, Ji LL (1995) Glutathione depletion in rested and exercised mice: biochemical consequence and adaptation. Arch Biochem Biophys 316:941–949

Lowe DA, Lund T, Alway SE (1998) Hypertrophy-stimulated myogenic regulatory factor mRNA increases are attenuated in fast muscle of aged quails. Am J Physiol 275:C155–C162

Lowe D, Thomas D, Thompson L (2002) Force generation, but not myosin ATPase activity, declines with age in rat muscle fibers. Am J Physiol 283:187–192

Martensson J, Meister A (1989) Mitochondrial damage in muscle occurs after marked depletion of glutathione and is prevented by giving glutathione monoester. Proc Natl Acad Sci USA 86:471–475

McBride TA, Gorin FA, Carlsen RC (1995) Prolonged recovery and reduced adaptation in aged rat muscle following eccentric exercise. Mech Ageing Dev 83:185–200

McBride JM, Kraemer WJ, Triplett-Mcbride T, Sebastianelli W (1998) Effect of resistance exercise on free radical production. Med Sci Sports Exerc 30:67–72

Meister A (1991) Glutathione deficiency produced by inhibition of its synthesis, and its reversal; applications in research and therapy. Pharmac Ther 51:155–194

Payne AM, Delbono O (2004) Neurogenesis of excitation-contraction uncoupling in aging skeletal muscle. Exerc Sport Sci Rev 32:36–40

Stevens ED (1996) Effect of phase of stimulation on acute damage caused by eccentric contractions in mouse soleus muscle. J Appl Physiol 80:1958–1962

Stevens ED, Faulkner JA (2000) The capacity of mdx mouse diaphragm muscle to do oscillatory work. J Physiol 522 (Pt 3):457–466

Tidball JG (2005) Inflammatory processes in muscle injury and repair. Am J Physiol Regul Integr Comp Physiol 288:R345–R353

Uchiyama S, Tsukamoto H, Yoshimura S, Tamaki T (2006) Relationship between oxidative stress in muscle tissue and weight-lifting-induced muscle damage. Eur J Physiol 452:109–116

Underwood EE (1970) Quantatative stereology. Addison-Wesley Publishing Co, Reading

Urso ML, Clarkson PM (2003) Oxidative stress, exercise, and antioxidant supplementation. Toxicology 189:41–54

Watanabe T, Sagisaka H, Arakawa S, Shibaya Y, Watanabe M, Igarashi I, Tanaka K, Totsuka S, Takasaki W, Manabe S (2003) A novel model of continuous depletion of glutathione in mice treated with L-buthionine (S, R)-sulfoximine. J Toxicol Sci 28:455–469

Weibel ER (1972) The value of stereology in analysing structure and function of cells and organs. J Microsc 95:3–13

Weibel ER (1974) Selection of the best method in stereology. J Microsc 100:261–269

Weibel ER (1975) Quantitation in morphology: possibilities and limits. Beitr Pathol 155:1–17

Willems ME, Stauber WT (2001) Force deficits after repeated stretches of activated skeletal muscles in female and male rats. Acta Physiol Scand 172:63–67

Zerba E, Komorowski TE, Faulkner JA (1990) Free radical injury to skeletal muscles of young, adult, and old mice. Am J Physiol 258:C429–C435